Meniscus solutions and shock dynamics for Marangoni-driven flows
Submitted for Presentation in ECS2005
The European Coating Symposium 2005

P. L. Evans, *and* ***A. Münch****
Institute for Mathematics, Humboldt University of Berlin, D-10099 Berlin, Germany
{pevans,muench}@mathematik.hu-berlin.de
**Also Weierstraß Institut für Angewandte Analysis und Stochastik, Berlin, Germany*

We consider a situation where a thin liquid film is driven from a reservoir up a substrate by a thermally induced Marangoni shear stress and investigate the meniscus that connects the film with the reservoir, as well as the wave dynamics near the contact-line. We identify two types of meniscus solutions, and show, via a phase space investigation of the third order ODE that governs the profile, when these solutions appear. The first type fixes the film thickness, hence the flow rate, and exists only below a critical inclination angle (measured with respect to the vertical position). The second yields thicker films and does not meter the flow. The rich wave dynamics near the contact-line involve non-classical (undercompressive) shocks and have themselves been the focus of intensive investigations in recent years. We summarise these results to demonstrate how the interplay of meniscus solutions and front dynamics determines the profile of the liquid surface. The discussion of the meniscus solutions carries over to the drag-out problem, for which in particular the dependence on the inclination angle has, to the best of our knowledge, not yet been systematically investigated.

1 Introduction

When a temperature difference is imposed along a substrate which has one end immersed into a reservoir of a liquid such as silicone oil, surface tension gradients can impose shear stresses which drag liquid up from the reservoir. This motion is opposed by gravitational forces acting to return liquid to the reservoir. Such a situation can arise in industrially important processes such as Marangoni drying [1] and microfluidic operations [2]. Experiments investigating this situation have been performed by Carles and Cazabat [3] for a vertical substrate and for tilted substrates [4, 5].

If σ denotes the surface tension of the coating, and x is a coordinate which increases with distance above the undisturbed level of the reservoir, then the surface shear stress driving the flow is $\tau = d\sigma/dx = (d\sigma/dT)(dT/dx)$. For a liquid with $d\sigma/dT < 0$, holding the upper end of the substrate at a lower temperature than at the meniscus ensures that $\tau > 0$. In this work, τ is assumed to be a positive constant along the entire substrate. A related situation, known as the withdrawal or "drag-out" problem, arises when the upward force is provided by dragging the substrate upward parallel to itself [6, 7]. The withdrawal situation displays some of the same features as seen here.

In this paper a model for Marangoni-driven flow of a thin film over a substrate with significant inclination is presented. In Section 3 we review recent results [8] describing meniscus solutions, that is, film profiles which satisfy the model in the meniscus and approach a layer of constant thickness above the meniscus. In the following section we examine the coating profile near its advancing front, based on a precursor model. The two independent pictures are combined in Sections 5 and 6 to give a coherent picture of film behaviour as the substrate inclination and precursor thickness are altered.

2 Lubrication model

Here we consider flow on a planar, tilted substrate, as shown in Figure 1. We denote the time-dependent film thickness profile by $h(x,t)$, where x measures distance up the substrate and t is time. The substrate is tilted at an angle α from the vertical. The (mean) surface tension of the

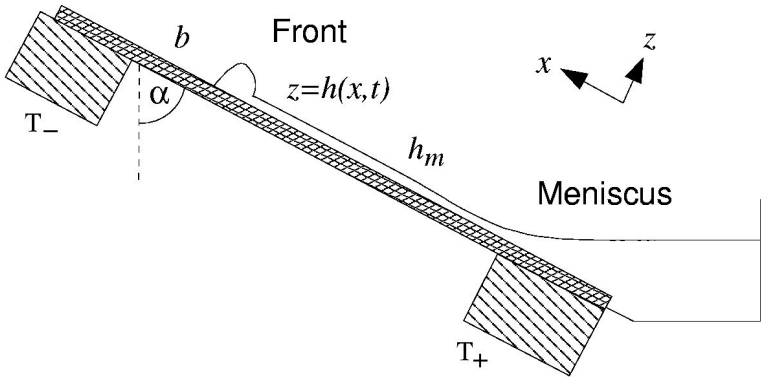

Figure 1: Thin film on a heated tilted substrate rising from a meniscus.

coating is σ, while its density ρ and viscosity μ are assumed to remain constant. Using familiar ideas from lubrication theory, an evolution equation governing *h(x,t)* may be obtained by exploiting the disparity between the thickness and substrate length scales [9]. We scale quantities in the thickness and substrate directions, and time, using

$$H=\frac{3\tau}{2\rho g\cos\alpha},\quad L=\left(\frac{3\sigma\tau}{2\rho^2 g^2\cos^2\alpha}\right)^{1/3},\quad t_0=2\mu\left(\frac{4\sigma\rho g\cos\alpha}{9\tau^5}\right)^{1/3}$$

respectively. The resulting dimensionless governing equation is

$$h_t+\Omega_x\left(h^2-h^3\right)_x=-\left(h^3\kappa_x\right)_x+D\left(h^3h_x\right)_x \tag{1}$$

where $\kappa=h_{xx}\left(1+\varepsilon^2h_x\right)^{-3/2}$ is the free surface curvature, and ε=*H*/*L*. Here the dimensionless parameter *D* is defined by [10]

$$D=\left(\frac{3\delta}{\cos^2\alpha}\right)^{2/3}\sin\alpha\ ,\ \text{where}\ \ \delta=\frac{\tau}{2\sqrt{\sigma\rho g}}\ .$$

Large values of *D* indicate that the normal component of gravity is important, and arise for large inclinations. The function *Ω(x)* is a dimensionless temperature profile which increases uniformly along the substrate (Ω_x = 1) except near the heaters, where *Ω* becomes constant, cutting off surface tension gradients there. Because of the relatively large tilt of the substrate, both the normal and tangential components of gravity are important, and these are retained in the equation above.

At the meniscus, the film is required to flatten so as to meet the undisturbed reservoir, so that in dimensionless units, $h \to -x/D$ as $x \to -\infty$. We are interested in the development of films on a notionally "clean" substrate, and suppose that initially a film of uniform very small thickness *b* covers the substrate. At the apparent contact line, we use a precursor model to avoid the singularity associated with a moving contact line [11] and require that $h \to b$ as $x \to \infty$.

For substrates sufficiently tilted away from the vertical, ε is much less than 1. It is then appropriate to replace *κ* by the approximate expression h_{xx} in the thin film region away from the reservoir. When in addition $\varepsilon \ll D$, it follows that $\varepsilon|h_x| \ll 1$ in the reservoir , and the approximate expression for curvature may also be used there. The latter condition is satisfied when $\tan\alpha \gg 1$. We set $\Omega_x \equiv 1$, requiring that as α is increased the position of the heater is moved further into the reservoir. In this way a uniform temperature gradient, and hence uniform shear stress, is imposed. Equation (1) then reduces to:

$$h_t + \left(h^2 - h^3\right)_x = -\left(h^3 h_{xxx}\right)_x + D\left(h^3 h_x\right)_x \tag{2}$$

A model equation very similar to (2), with h^2 replaced by h in the flux term on the left, can be derived for the withdrawal problem. We are concerned with the behaviour of solutions of (2) subject to the boundary conditions above. This model is influenced by just two parameters, D, and the precursor layer thickness, b. A particular combination of these parameters determines the structure of the climbing film.

Solutions of (2) typically have two distinct parts, a meniscus and a moving wave structure consisting of one or more advancing waves. Near the reservoir, the meniscus part settles into an equilibrium solution with thickness approaching some constant value h_m. At the apparent contact line is an advancing travelling wave which we refer to as the "advancing front". Behind it may be additional waves, which together with the advancing front make up the moving wave structure. A good guide to the behaviour of the complete film comes from examining what happens considering the two parts of the film independently. We do this in the following two sections, then describe the possible structures for the entire film.

3 Meniscus

In previous work [8] we examined how coating profiles near the meniscus can be matched to a flat region of thickness h_m, and we summarise our results here. Two distinct types of profiles were found by considering the third-order ordinary differential equation (ODE) describing stationary solutions of (2). For a given D somewhat smaller than $D_M \approx 0.8008$, a stationary meniscus solution can be found for which $h_m < 2/3$, for one special value of $h_m = h_B(D)$. For the same value of D, meniscus solutions can also be found with $h_m \geq h_T(D)$, where h_T is the larger positive root of $f(h) = f(h_B)$, and $h_T > 2/3$. We denote the solution with $h_m = h_B$ as a Type I meniscus solution. These have a thickness profile which monotonically decreases with x. When the film has $h_m \geq h_T$, we call this a Type II solution. Type II solutions typically have a depression or dimple in the meniscus region, and their thickness approaches h_m by a damped oscillation, associated with a complex conjugate pair of eigenvalues in the characteristic equation of the ODE (for $D < 0.6964$). These are shown in Figure 2. A somewhat similar situation arises in the withdrawal problem, where for rising film flows, a layer of thickness increasing with capillary number can be produced, while falling films with the same flux are thicker, and have oscillating profiles [12].

For $h_m = h_T(D)$, our earlier analysis shows that there are an infinite number of steady solutions. Similarly, for h_m in an range of values near but not equal to $h_T(D)$, there are a finite number of multiple solutions. Our numerical simulations suggest that every second one of these solutions is stable to in-plane disturbances. (We do not discuss these further here; they are considered in an upcoming paper [13].)

The pair of values h_B and h_T both become closer to 2/3 as D approaches D_M. For $D > D_M$, no Type I meniscus profiles exist, and a steady meniscus profile can be found for any $h_m > 2/3$. Plotting h_B and h_T against D forms a structure, shown in Fig. 3(a), we call the "meniscus wedge". The shape of the meniscus wedge does not, of course, depend on properties of the contact region, such as b.

4 Moving wave structure

The advancing front has been quite widely studied. Münch presented a family of travelling wave profiles for the advancing front, obtained as D is varied. [14]. These profiles have thickness approaching a constant left state value h_w away from the contact line, and have $h \to b$ as $x \to \infty$. They included compressive (Lax) waves and double wave structures [4, 10]. The compressive waves have a characteristic capillary ridge connecting the left state to the precursor layer. One double wave structure (a "double shock structure") consists of a leading wave, which is undercompressive and has a left state h_{uc} and right state b, and a trailing wave which is compressive, with left state $h_w < h_{uc}$ and right state h_{uc}. Another double wave structure

(a "rarefaction fan-undercompressive front combination") is formed by the combination of a rarefaction wave, in which the film thickness smoothly decreases from $h_w > h_{uc}$ until reaching h_{uc}, and an undercompressive leading wave. In this structure, the two waves are separated by a plateau of thickness h_{uc} which depends on both b and D. They both have a positive speed, and so move up the substrate over time. However, the undercompressive wave moves faster than the compressive wave of the rarefaction fan, and so the width of the plateau grows over time.

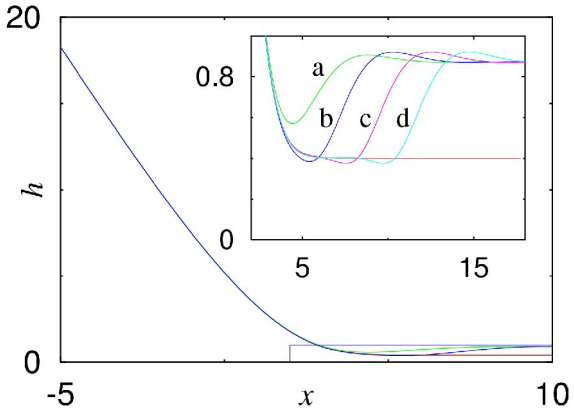

Figure 2: Meniscus structures for D=0.322. Red line is a Type I meniscus; those labelled 'a' to 'd' are Type II menisci.

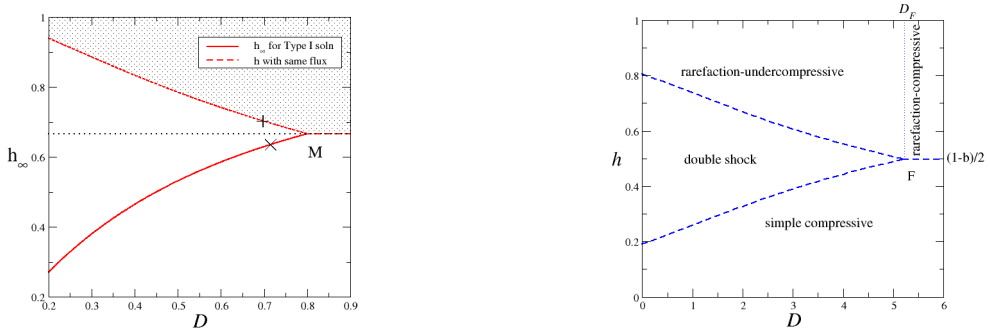

Figure 3: (a) Meniscus wedge. (b) Front wedge diagram for b=0.005.

These results may be summarised in a two-dimensional "front wedge" diagram that displays, for each D, the values of h_w where the different types of wave or waves connecting this state to the precursor right state exist. In the (D, h_w) plane, the boundaries between these different regions form a wedge-like shape, shown in Figure 3(b) for the precursor thickness b=0.005. This shape is defined by $h_w = h_{uc}(D,b)$ (at the upper edge) and $h_w = 1 - h_{uc} - b$ (lower edge).

The two sides of the wedge, together with the extension of the wedge's apex $\{(D, h): D>D_F, h=(1-b)/2\}$ and the line $\{(D, h): D=D_F, h>(1-b)/2\}$, divide the plane into four regions. The region in which a (D, h_w) pair lies in the diagram indicates which wave structure will arise for this combination. For relatively small values of h_w, a simple compressive wave, with a capillary ridge, arises. Within the wedge, the compressive-under-compressive double shock structure described above occurs. For large values of h_w, one obtains double wave structures with rarefaction fans. These are a rarefaction fan-undercompressive front combination when $D<D_F$

and $h_w > h_{uc}$. To the right of the apex ($D > D_F$) are found solutions with a rarefaction fan and leading generalised Lax shock.

The shape and position of the front wedge on a (D, h_w) diagram changes with b, because h_{uc} depends on b. The apex of the wedge (F in the figure) is located at ($D_F(b)$, $(1-b)/2$), and moves to smaller D as b increases.

5 Combined behaviour

The question arises is now: how can the above information about the meniscus and front structures be combined? When the coating has had sufficient time to develop, so that the contact line is far from the reservoir, the meniscus profile may approach an approximately steady state. In this case, the film thickness above the meniscus approaches a suitable h_m for which a Type I or Type II meniscus exists, and this thickness is the left state value h_w used to determine the front structure.

An overview of the possible combinations of the different types of meniscus and wave structures can be obtained by superimposing the two wedge diagrams. In many cases, this suggests more than one possible outcome for a given D and b. For example, if $D < D_M$, wave structures can be found to connect to either a Type I or a whole range of Type II menisci. By using dynamic considerations, we can in many cases determine which film profile evolves from monotone initial data such as

$$h(x,0) = \begin{cases} D^{-3/2}\left(\exp\left(D^{1/2}x\right) - D^{1/2}x - 1\right) + b & \text{for } x \le 0, \\ b & \text{for } x > 0, \end{cases} \tag{3}$$

representing a uniform thin precursor layer on a substrate which is partially immersed into the reservoir, where the meniscus is free of surface tension gradients. These predictions are verified using simulations of the time-dependent PDE (2).

5.1 Thin precursor layer

The most important parameter range is for small b, i.e., a very thin precursor layer. In this case, D_F is large. The upper branch of the front wedge makes intersections with the curve $h_T(D)$ and the line $h = 2/3$, as seen in Figure 4, for $b = 0.005$. This arrangement of the wedges continues until $h_{uc}(D_M, b) = 2/3$; this happens for $b \approx 0.0202$.

When D is small, but still large enough that $h_B > b$, the film meniscus must be of Type I. This continues until $D = D_I$ where the lower sides of the two wedges intersect in the (D, h) diagram. For, suppose the meniscus were of Type II, with a right state thickness $h_m \ge h_T$. In this range of D, h_T in turn is larger than h_{uc}. A connection from h_m to the precursor would involve a rarefaction fan followed by an undercompressive wave joining to b. The left part of the rarefaction fan would then have negative speed, and therefore would fall back into the meniscus. Hence such a solution cannot persist.

On the other hand, if the meniscus is of Type I, then $h_m = h_B < 1 - h_{uc} - b$, and a simple compressive connection to the precursor is possible. This is connected by a flat film to a steadily advancing front. The left state of the advancing front and the right state of the meniscus are identical in this case, since the two are directly connected. Dynamical simulations for $D = 0.1021 < D_I$ and $b = 0.005$ (Example 1 of Ref. [8], also shown in Fig. 5(a)) confirm that this combination of Type I meniscus and a simple compressive wave occurs. The flat region thickness is metered by the meniscus in this case, in the sense that it is determined by D, and independent of b.

When D exceeds D_I, the Type I meniscus thickness $h_B(D) > 1 - h_{uc} - b$. In place of a simple compressive connection, a Type I meniscus must now connect to a double shock structure. As

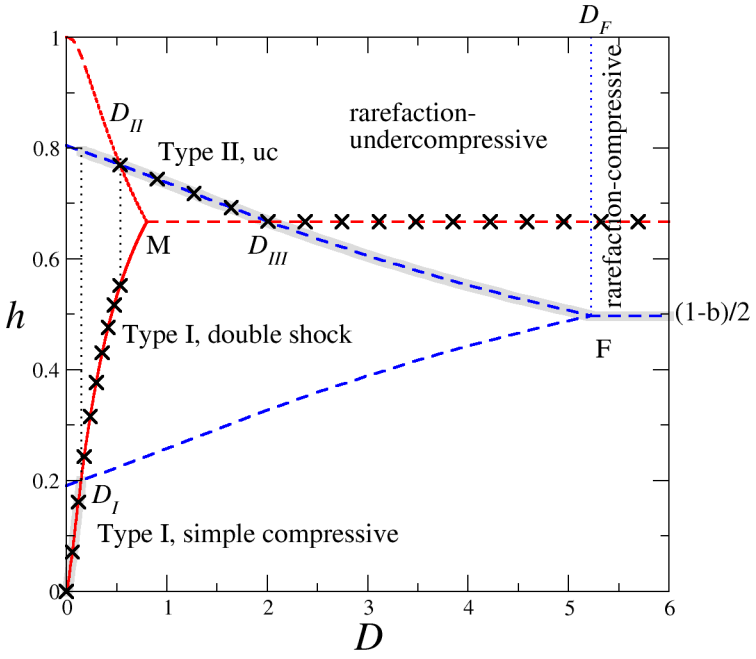

Figure 4: A (D, h) diagram showing the front wedge for b=0.005 (blue) and the meniscus wedge (red).

in the previous case, a Type II meniscus is still not possible, as $h_T > h_{uc}$ while $D < D_{II}$. Now the left state of the advancing front is the undercompressive wave height h_{uc}. The flat region ahead of the meniscus, with thickness h_B, is connected to h_{uc} by the trailing compressive part of the double wave structure. This trailing shock moves upwards, but somewhat slower than the advancing front. In the (D, h) diagram, Figure 4, the graph of $h_B(D)$ enters the front wedge, and the shaded line jumps to h_{uc} at $D = D_I$, separating from the line portion emphasised by crosses. (In this discussion we omit a complication arising from the existence of multiple compressive waves or a double shock being possible at the same (small) value of D, when h is slightly larger than $1 - h_{uc} - b$ [14]. For monotone initial conditions such as (3), the effect of this is to slightly shift the transition from compressive fronts to double shocks to a value D'_I slightly greater than D_I.) Double shock structures continue to develop until $D = D_{II}$, the value of D where $h_{uc} = h_T$ and the upper sides of the two wedges cross. For b=0.005, D_{II} = 0.535. A double shock structure moving up the substrate is shown for D=0.322 in Example 2 of Ref. [8], and also in Fig. 5(b).

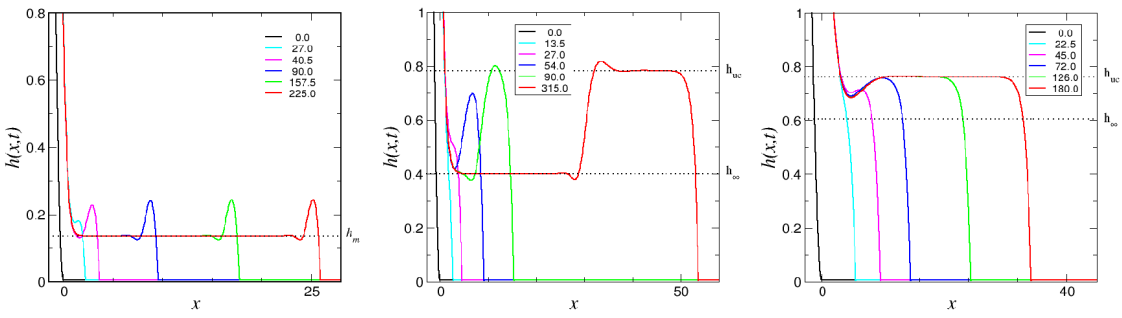

Figure 5: Numerical solutions for increasing values of D. From left to right, (a) D=0.0121, (b) D=0.3220 and (c) D=0.6424, with b=0.005 in each case.

For $D_{II} < D < D_{III}$, h_{uc} is larger than h_T and so it lies in the region where Type II meniscus solutions are possible. Hence a direct undercompressive shock connection from a Type II meniscus to the precursor is possible. (The existence of multiple Type II solutions for h near h_T means that one or more Type II solution is also available for matching to h_{uc} via a direct connection for values of D slightly below D_{II}.) These continue until $D = D_{III}$, defined by where $h_{uc} = 2/3$; for b=0.005, $D_{III} = 2.025$. For $D < D_{III}$, h_{uc} is larger than 2/3. Thus we can rule out connections involving intermediate waves as follows. Only shocks can connect to h_{uc} from below, and these would have a negative speed. (Characteristics for the left and right state would cross, ruling out a rarefaction fan). Similarly, any wave connection from above must be a rarefaction fan, all parts of which would also have a negative speed.

As a result, the only structure possible is a Type II meniscus connecting directly to a flat state with thickness h_{uc}. This flat state is the left state of an undercompressive shock connection to the precursor. The right state of the meniscus and the left state of the advancing front are again identical, and in Fig. 4 the lines marked by crosses and shading coincide. It is notable that in this range of D, the thickness of the flat region, h_{uc}, is determined by the precursor thickness, not by the meniscus. We therefore refer to these structures as "front controlled". This situation in this range is exactly what is observed for Example 3 from Ref. [8], and in Fig. 5(c), where D=0.6424. (Once again, this description has to be qualified slightly, due to the existence of Type II menisci somewhat below h_T [8]. This complicates the transition from Type I to Type II meniscus around $D = D_{II}$.)

For the small values of D considered so far, our "separation assumption" is justified *a posteriori*, as dynamical simulations confirm that there is in fact a distinct flat region between the meniscus and the wave structure. For larger D, this is not so. As D increases beyond D_{III}, the height of the left state for an undercompressive front h_{uc} drops below h=2/3. Now there can be no direct connection between meniscus and front. All available meniscus profiles have h_m larger than h_{uc}, so an intermediate wave is needed to span the thickness gap. From the front wedge part in Figure 3(b), we see that the resulting wave structure must be a rarefaction-undercompressive wave combination.

No flat film can emerge between the meniscus and the rarefaction wave with a thickness $h_m=h_w$ strictly larger than 2/3, since the portions of the rarefaction wave larger than 2/3 would have a negative characteristic speed. Instead the meniscus evolves into a shape that is the limiting profile of all the Type II menisci, while the portions of the film between 2/3 and h_{uc} tend to the profile of rarefaction wave with left state 2/3. Since the characteristic speed at h=2/3 is exactly zero, the rarefaction wave never completely separates from the meniscus, but as it gets increasingly stretched, the film thickness at a any fixed position x in front of the meniscus eventually tends to 2/3. We call the emerging limiting meniscus profile with thickness h_m=2/3 a *generalised* Type II meniscus, in analogy to the terminology for Lax waves.

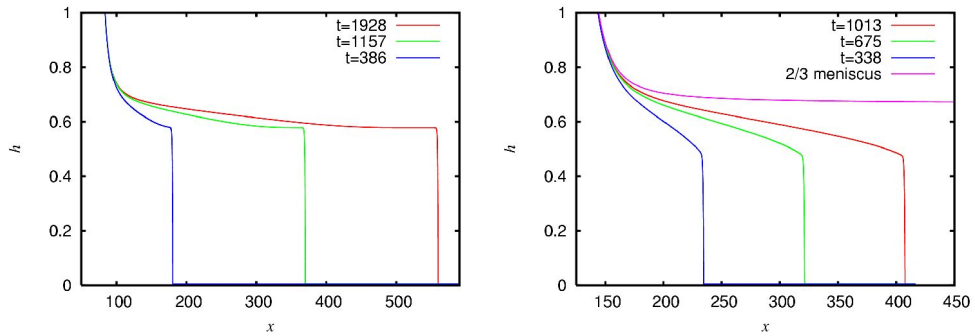

Figure 6: For large D and b=0.005 a Type I meniscus connects to the advancing front via a rarefaction fan. (a) D=3.5. (b) D=6.

This situation is indicated in Figure 4, where for $D > D_{III}$, the crossed and shaded lines part again. The former line lies at the boundary of the Type II regime, while the latter follows the

upper edge of the front wedge. Dynamical simulations with D=3.5 confirm our picture (Figure 6(a)). At long times, the film to the left of the advancing front forms a flat plateau with thickness equal to h_{uc} = 0.5783. (This value was obtained by solving the travelling wave ODE a [10, 14]). At an increasing distance from the advancing front, the film profile steepens slightly to a rarefaction wave, which blends over into the meniscus.

When D increases further, h_{uc} decreases, and the difference between the speed of the undercompressive wave and the left characteristic speed of this wave also decreases. They become equal when $D = D_F$ and $h_{uc} = (1–b)/2$ at the apex of the front wedge. For b=0.005, D_F = 5.227. For the largest D, in excess of D_F, the possible wave structures are those that are permitted according to classical shock theory.

Again, the meniscus profile tends to a generalised Type II meniscus, and it must connect to a rarefaction fan with left state 2/3. The rarefaction wave now connects directly to the advancing front, which connects in turn to b. The characteristic speed of the thickness $(1–b)/2$ where the two structures connect is identical to the shock speed. The leading shock is therefore a (compressive) generalised Lax wave, and there is neither the flat region of thickness h_{uc} nor the steep shock front which were visible when D=3.5. This is seen in a dynamical simulation for D=6 in Figure 6(b). Instead the rarefaction fan expands over time, always stretching from the meniscus to the advancing front. The front is a generalised Lax shock, and connects to the rarefaction fan via a rounded corner at thickness $h=(1–b)/2$ = 0.4975. Also shown in the figure us the generalised Type II meniscus profile approached when the front has moved far up the plate.

5.2 Thicker precursors

As b is increased, the front wedge shrinks, and overlaps with the meniscus wedge in different arrangements, altering the way in which the meniscus and front can interact. For b> 0.0202 the upper branch of the front wedge intersects the lower branch of the meniscus wedge (so there are D values for which $h_B = h_{uc}$) until b > 0.2338. Within this range of D, it is possible for a Type I meniscus to join to a double shock structure as in Section 5.1, or (via a rarefaction fan) to an advancing undercompressive front. For still b larger than this value, the front wedge lies entirely within the meniscus wedge, and undercompressive fronts are no longer possible. However we expect that such precursors are unlikely to be encountered in practice, and do not discuss them in further detail here.

6 A catalogue of behaviours

Using the methods of Section 4, we can classify the behaviour expected for a large part of (D, b) parameter space. The distinct behaviours seen are shown in Figure 7. Region boundaries are found by computing values of $h_{uc}(D,b)$, $h_B(D)$ and $h_T(D)$, and the expected behaviour is confirmed in each region by numerical simulations at multiple points.

Three types of solutions, having only a direct connection between the meniscus and advancing front shock(s), only exist for small D or b. These include a Type I meniscus, connected by a flat region of thickness $h_m = h_B$, joining either a Lax compressive front with a small capillary ridge (denoted “T1+Lax” in Figure 7), or a double shock structure (“T1+ds”). The double shock advances up the substrate over time, as shown in Figure 5(b). A Type II profile, with a flat region thickness set by an advancing undercompressive front (“T2+uc”) is also possible. For a fixed value of D, one of these separated configurations can only arise when a sufficiently thin precursor is present.

For larger D and b the coating profile develops a rarefaction fan (shown as “rf” in the Figure 7 labels) and there is then no clear separation between the meniscus and the front. For the largest D > max(D_F, D_M), the meniscus is of generalised Type II, and the advancing front is a generalised Lax wave (labelled “2/3+rf+gL”), or if $D_F < D < D_M$ then the meniscus is of Type I

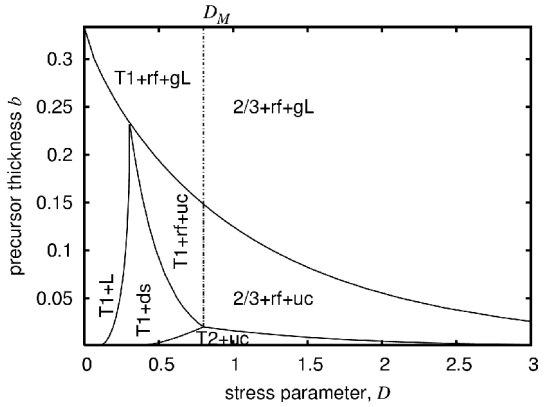

Figure 7: Classification of film behaviour.

("T1+rf+gL"). If the precursor layer is thin enough, the front is undercompressive (indicated as "T1+rf+uc" and "2/3+rf+uc").

7 Concluding remarks

This paper has presented a synthesis of knowledge of the film on a heated tilted substrate both near a meniscus and at an advancing front. Combining this data, and confirming with dynamical simulations, we identified the possible behaviours for the entire film. Our results are summarised in Figure 7, which shows the range of behaviours found for different choices of D and b. We find that profiles with extended flat regions and with rarefaction fans are possible.

Our discussion has a few limitations: our restriction to small ε means the model here cannot describe substrates which are nearly vertical, for additional curvature terms then become significant. In this limit h_B is known to approach a finite non-zero value [3, 8, 9]. We have also neglected some subtleties related to the existence of multiple Type II solutions for h near h_T.

Our analysis for the thermally-driven coating is in the spirit of earlier work on the withdrawal problem. The possibility of multiple values for the thickness of a fully-developed infinitely-long flat region above the meniscus for certain inclination ranges was raised by Wilson [6] for the withdrawal problem; here we find multiple solutions for the meniscus for $D < D_M$. Hocking [7] used the idea of matching meniscus and contact line solutions to show how conditions at the contact region can explain Wilson's difficulties at low plate inclination. Below a certain capillary number, which increases with contact angle, the coating thickness depends on contact angle, with a transition region before the film meets the meniscus. Using a similar approach, we find that for small values of D, a theory neglecting the contact line is applicable, with the contact region adapting to the thickness chosen by the meniscus, while for large D, the situation is reversed. The smaller thickness expected for a steady meniscus, h_B is not observed; instead the thickness h_T is set by contact line conditions.

One significant difference from the withdrawal problem is that the flux function there, $h - h^3$, is not convex for positive h, while that of the present problem, $h^2 - h^3$ is convex for $h < 1/3$. Thus in the withdrawal problem there can be no undercompressive shocks as are observed at the fronts here [14].

We anticipate that the modelling here can be confirmed by experimental data. Typical values of δ are small, less than 0.01 [5, 15] so obtaining large values of D is difficult. However the most important transitions, from Type I, to double shock, to Type II, occur at only moderate D, and so should be reasonably accessible.

Acknowledgements

This work was supported by the DFG Research Centre Matheon (Project C10) in Berlin. AM was also supported by a DFG Heisenberg Fellowship.

References

1. Matar, O. K. and Craster, R. V., 2001, Models for Marangoni drying, *Phys. Fluids*, **13**, 1869–883.
2. Haskett, R. P., Witelski, T. P. and Sur, J., (2005), Localized Marangoni forcing in driven thin films, *Physica D*, available online 18 July 2005.
3. Carles, P. and Cazabat, A.-M., 1993, The thickness of surface-tension-gradient-driven spreading films, *J. Colloid Interface Sci.*, **157**, 196–201.
4. Bertozzi, A. L., Münch, A., Fanton, X., and Cazabat, A.-M., 1998, Contact line stability and "undercompressive shocks" in driven thin film flows, *Phys. Rev. Lett*., **81**, 5169–5172.
5. Schneemilch, M. and Cazabat, A.-M., 2000, Shock separation in wetting films driven by thermal gradients, *Langmuir*, **16**, 9850–9856; Wetting films in thermal gradients, *Langmuir*, **16**, 8796–8801.
6. Wilson, S. D. R., 1982, The drag-out problem in film coating theory, *J. Engrg. Math*., **16**, 209–221.
7. Hocking, L. M., 2001, Meniscus draw-up and draining, *Euro. J. Appl. Math.*, **12**, 195–208.
8. Münch, A. and Evans, P. L., 2005, Marangoni-driven liquid films rising out of a meniscus onto a nearly-horizontal substrate, *Physica D*, available online 18 July 2005.
9. Münch, A., 2002, The thickness of a Marangoni-driven thin liquid film emerging from a meniscus, *SIAM J. Appl. Math*., **62**, 2045–2063.
10. Bertozzi, A. L., Münch, A, and Shearer, M., 1999, Undercompressive waves in driven thin film flow, *Physica D*, **134**, 431–464.
11. Huh, C. and Scriven, L. E., 1971, Hydrodynamic model of steady movement of a solid/liquid/fluid contact line, *J. Colloid Interface Sci*., **35**, 85–101.
12. Kheshgi, H. S., Kistler, S. F., and L. E. Scriven, 1992, Rising and falling film flows: viewed from a first-order approximation, *Chem. Eng. Sci.*, **47**, 683–694.
13. Evans, P. L. and Münch, A., 2005, Dynamics of a surface-tension-gradient-driven liquid film rising from a reservoir onto a substrate, under consideration for *SIAM J. Appl. Math.*
14. Münch, A., 2000, Shock transitions in Marangoni-gravity driven thin film flow, *Nonlinearity*, **13**, 731–746.
15. Mukhopadhyay, S and Behringer, R., personal communcation.